Joint population pharmacokinetic analysis of zidovudine, lamivudine, and their active intracellular metabolites in HIV patients

Caroline Bazzoli, Henri Bénech, Elisabeth Rey, Sylvie Retout, Dominique Salmon, Xavier Duval, Jean-Marc Tréluyer, France Mentré

Population joint pharmacokinetic analysis of zidovudine, lamivudine and their active intracellular metabolites in HIV patients

C. Bazzoli[1, 2*], H. Bénech[3], E. Rey[4], S. Retout[1], D. Salmon[5],

X. Duval[1, 6], J. M. Tréluyer[4], F. Mentré[1] and the COPHAR2- ANRS 111 study group

[1] UMR 738, INSERM and Université Paris Diderot, Paris, France;

[2] Laboratoire Jean Kuntzmann, Université de Grenoble et CNRS, Grenoble, France;

[3] CEA, iBiTecS, Service de Pharmacologie et d'Immunoanalyse, Gif sur Yvette, France;

[4] Université Paris Descartes ; AP-HP ; Groupe Hospitalier Cochin – Saint-Vincent de Paul ; Service de Pharmacologie Clinique ; Inserm U663 ;

[5] Université Paris 5, AP-HP, Hôpital Cochin, Service de Médecine Interne, Paris, France;

[6] CIC 007, Hôpital Bichat, Paris, France ;

Running title: Joint population PK for AZT/AZT-TP and 3TC/3TC-TP

* **Corresponding author (present address):**

Caroline Bazzoli,

Laboratoire Jean Kuntzmann,

Université de Grenoble et CNRS,

51 rue des Mathématiques,

F-38041 GRENOBLE cedex 9

Email: bazzolic@iut2.upmf-grenoble.fr

Abstract

The population pharmacokinetic parameters of AZT and 3TC and their active intracellular metabolites were described from 75 naïve HIV infected patients receiving oral combination of AZT and 3TC twice daily, as part of their multitherapy treatment in the COPHAR2 – ANRS 111 trial. Four blood samples per patient were taken after two weeks of treatment to measure the concentration at steady state. Plasma AZT and 3TC concentrations were measured in 73 patients among those 62 patients had measurable intracellular AZT-TP and 3TC-TP concentrations. For each drug, a joint population pharmacokinetic model was developed and we investigated the influence of different covariates. We then studied correlations between mean plasma and intracellular concentrations of each drugs. A one compartment model with first order absorption and elimination best described plasma AZT concentration, with an additional compartment for intracellular AZT-TP. A similar model but with zero order absorption was found to adequately described concentrations of 3TC and its metabolite 3TC-TP. AZT and 3TC half-lives were 0.81 h (94.8%) and 2.97 h (39.2%), respectively whereas intracellular half-lives for AZT-TP and 3TC-TP were 10.73 h (69%) and 21.16 h (44%), respectively. We found particularly a gender effect on the apparent clearance of AZT as well as on mean plasma and intracellular concentrations of AZT, which were significantly higher in females than in males. Relationships between mean plasma and intracellular concentration were also highlighted both for AZT and for 3TC. Simulation with the model of plasma and intracellular concentrations for once versus twice daily regimens suggested that daily dosing regimen with double doses could be appropriate.

INTRODUCTION

Zidovudine (AZT) and lamivudine (3TC) are common antiretroviral drugs for treatment of human immunodeficiency virus (HIV) that causes Acquired Immunodeficiency Syndrome (AIDS). AZT and 3TC are nucleoside reverse transcriptase inhibitors (NRTIs), which are often used in highly active antiretroviral therapy (HAART) either associated to one protease inhibitors (PIs) boosted with ritonavir in general or with non-nucleoside reverse transcriptase inhibitor. The 2009 recommendations of the World Health Organisation recommended the use of AZT as a preferred first line therapy option, a less toxic alternative as the use of stavudine (38). As AZT and 3TC are frequently prescribed together, they are combined into one tablet (Combivir®).

All NRTIs undergo a series of three sequential phosphorylation reactions producing monophosphates, diphosphates, then triphosphates (TP) within the cell. AZT and 3TC are thus metabolised intracellularly to their active metabolite (AZT-TP and 3TC-TP, respectively), which block DNA synthesises by reverse transcriptase inhibition and chain termination. These active moieties are the determinants of the efficacy and of the toxicity of AZT and 3TC. Several studies have demonstrated that the antiviral activity of NRTIs does not always correlate with plasma concentrations of the parent nucleoside, but with the intracellular concentration of their metabolites (1, 3, 15, 17, 25, 33). The review performed by Bazzoli et al. (6) reports in more details these findings for NRTIs as well as for other antiretroviral drugs.

Assaying adequately the intracellular concentrations of antiviral drugs is still a major technical challenge, together with the isolation and the count of peripheral blood mononuclear cells (PBMCs) (6). That is why, most studies with intracellular measurements in patients of AZT-TP and or 3TC-TP, have often been carried out in relatively few patients with observations mostly at single time points. Even if population approaches seem to be more adequate to analyse sparse pharmacokinetic data, no population pharmacokinetic study has yet been performed from

intracellular measurement of AZT-TP and 3TC-TP, only population pharmacokinetic analyses on plasma have been published.

The COPHAR 2-ANRS 111 trial is a multicentre, non-comparative pilot trial of early therapeutic drug-monitoring in HIV-positive patients naïve for PI-containing HAART (16). Patients received a combination of two NRTIs plus one PI as antiretroviral therapy. Population PK analyses of the data from the nelfinavir group and the indinavir boosted with ritonavir group, obtained in this trial, were performed to evaluate the impact of genetic polymorphisms on nelfinavir and indinavir pharmacokinetic and the link between concentrations and short term efficacy (10, 21). A sub-study of the COPHAR 2 ANRS111 trial consisted of measuring plasma and intracellular concentrations of AZT and 3TC in patients whom treatment contained AZT and 3TC as NRTIs with the PI. In the present study, we focused on the simultaneous population analyses of concentration data for AZT and 3TC and their respective intracellular active metabolite, through the development of joint population models. Integrated modelling of parent-metabolite pharmacokinetics provides reliable estimate of metabolite parameters and their intersubject variability. We then investigated the influence of different covariates on the pharmacokinetic parameters of these both models. Last, we explored relationships between mean plasma concentrations of both drugs as well as between mean intracellular concentrations of both metabolites. We also studied correlations between plasma and intracellular concentrations for both drugs and with the final covariates found for each model, respectively.

MATERIALS AND METHODS

Patients and study design

The objective of the COPHAR2-ANRS 111 trial was to assess the benefit of pharmacological advice based on trough plasma concentrations of PI (Details can be found in (16)). Patients initiated a HAART treatment containing a combination of at least three drugs: one PI (indinavir/ritonavir or lopinavir/ritonavir or nelfinavir), plus two NRTIs (AZT (300 mg) /3TC (150 mg) (Combivir®) b.i.d or d4T (40mg) /3TC (150 mg) b.i.d). A sub-study of the clinical trial has been performed to establish the pharmacokinetics of AZT and 3TC and of their intracellular moieties in patients receiving this dual combination.

Patient eligibility criteria were HIV infection, age over 18 years, no previous treatment with a PI regimen, a plasma HIV RNA level above 1000 copies/ml, naive to antiviral treatment or else a genotypic resistance test not indicating more than two major mutations. The main non-inclusion criteria were: concomitant use of drugs interacting with NRTIs and PIs; treatment of HIV infection with IL-2, interferon α, or vaccine; treatment with laxatives; renal failure (creatinine clearance <30 mL/min); cardiac dysfunction, liver dysfunction (prothrombin test <60% or liver cirrhosis); ongoing chemotherapy; pregnancy; ongoing acute opportunistic infection or cancer.

The Ethical Review Committee of Bicêtre Hospital, Paris, France reviewed and approved the study protocol. All participants provided written informed consent. No dose adaptation was performed from week 0 and to week 4.

After two weeks of treatment (W2), four blood samples per patient were taken to measure the plasma concentration at steady state before and at 1, 3, 6 h after drug administration. This design was developed for the study of PI pharmacokinetics and AZT and 3TC concentrations were assessed in these samples. Regarding intracellular measurements, patients receiving AZT/3TC were sampled before and at 3 h after drug intake, additional blood samples were also collected at 1 h and 6 h for patients in the nelfinavir group. Adherence was evaluated at W2 by means of a validated auto-

questionnaire (11) and patients were classified as adherent when reporting no shift in their treatment schedule during the last 4 days and non-adherent otherwise.

Analytical method

Plasma concentrations were centralized and measured at the end of the study in the department of clinical pharmacology of the Cochin Hospital, Paris, France with a specific high-performance liquid chromatography method and reported in mg/L. Lower limits of quantification (LOQ) were 0.05 mg/L for AZT and 0.02 mg/L for 3TC.

Intracellular concentrations of NRTIs triphosphate metabolites were measured in the isolated peripheral blood mononuclear cells (PBMCs) using a liquid chromatography-tandem mass spectrometry (LC-MS/MS)(7, 13) at the Pharmacology and Immunoanalysis Unit of the CEA, Gif sur Yvette, France. Isolation of PBMCs is the first step before analyzing the intracellular concentrations of NRTIs. PBMCs were isolated either using conventional Ficoll gradient centrifugation or using cell preparation tubes (CPTs) (from Becton Dickinson). Cells were washed three times with a saline solution at +4°C, cells were stored at -80°C until extracted. Then, the intracellular concentrations were extracted from cells using a mixture of Tris HCl (0.05M PH 7.4) / methanol:30/70 (v/v) buffer (stored at -20°C).Cells were manually lysed (by scraping and vortexing). The supernatants were transferred and evaporated until a volume of 120µL was obtained, 40µL were then injected into the LC-MS/MS system. The chromatographic step was performed on a C18 reversed phase column with a mobile phase containing acetonitrile and a buffer of ammonium formate and 1.5-dymethylhexylamine as volatile counter-ion. Detection was achieved in tandem mass spectrometry after electrospray ionization in the negative mode. All values were then divided by the number of PBMC to obtain the concentration in fmol/10^6 cells.

For the present study intracellular concentrations in fmol/L were transformed in mg/L considering that one mole of AZT-TP and 3TC-TP were equal to 507g and 469g respectively and the PBMC volume approximated by 0.2 pL (12, 32). There is no standard methodology to set a LOQ for these measurements since it would depend both on the quantification of the intracellular compound and on the count of PBMC.

Population pharmacokinetic modelling

Two joint population pharmacokinetic models were developed in order to simultaneously describe the pharmacokinetics of AZT and 3TC and their active metabolites, respectively. Model fitting and estimation of the population parameters were performed using the SAEM algorithm for nonlinear mixed effects models implemented in the MONOLIX software version 2.3 (www.monolix.org). Plasma and intracellular concentrations were assumed at steady state with a dosing interval of 12 h. The through concentration was that measured the day before drug intake and the delay since last dose intake was used.

As suggested by previous analysis, we used a one compartment model with first order absorption and elimination to describe plasma AZT concentrations (29) (Fig 1). A compartment for AZT-TP was added, which was the link to the AZT compartment with a first order metabolism rate constant k_m, as it was assumed that there is no first pass effect. The parameters of this model are F, the bioavailability, the volumes of distribution of AZT and its metabolite AZT-TP (V and V_m), the first order absorption rate constant for AZT k_a, the metabolism rate constant k_m and the elimination rate constant for AZT and for AZT-TP (k_e and k_{em}, respectively). The equations of this model at steady state with a dosing interval τ are:

$$C_{AZT}(t) = \frac{F Dose\, k_a}{V(k_a - k)}\left(\frac{e^{-kt}}{1-e^{-k\tau}} - \frac{e^{-k_a t}}{1-e^{-k_a \tau}}\right)$$

$$C_{AZT-TP}(t) = \frac{FDose\, k_m k_a}{V_m}\left(\frac{e^{-kt}}{(k_a-k)(k_{em}-k)(1-e^{k\tau})} + \frac{e^{-k_a t}}{(k-k_a)(k_{em}-k_a)(1-e^{k_a\tau})} + \frac{e^{-k_{em}t}}{(k_a-k_{em})(k-k_{em})(1-e^{k_{em}\tau})}\right)$$

where C_{AZT} is the plasma concentration of AZT, $C_{AZT\text{-}TP}$ the intracellular concentrations of the metabolite AZT-TP and $k=k_e+k_m$.

An identical model but with a zero order absorption (*Tk0*) was applied to adequately described plasma concentrations of 3TC and intracellular concentrations of the metabolite 3TC-TP (Fig 1). The equations of this model at steady-state are described as follows:

$$C_{3TC}(t) = \begin{cases} \dfrac{FDose}{Tk0\,V\,k}\left(1-e^{-kt}\right) + e^{-k\tau}\dfrac{(1-e^{-kTk0})(e^{-k(t-Tk0)})}{1-e^{k\tau}} & if\ t \le Tk0 \\ \dfrac{FDose}{Tk0\,V\,k}\dfrac{\left(1-e^{-kTk0}\right)e^{-k(t-Tk0)}}{1-e^{-k\tau}} & if\ not \end{cases}$$

$$C_{3TC-TP}(t)\begin{cases} \dfrac{FDose\, k_m}{Tk0\,V_m\left(k-k_{em}\right)}\left(\dfrac{1}{k}\left(\left(e^{-kt}-1\right)+e^{-k\tau}\dfrac{\left(e^{-kTk0}-1\right)e^{-k(t-Tk0)}}{(1-e^{k\tau})}\right)\right. \\ \left. +\dfrac{1}{k_{em}}\left(\left(1-e^{k_{em}t}\right)+e^{-k_{em}\tau}\dfrac{\left(1-e^{-k_{em}Tk0}\right)e^{-k_{em}(t-Tk0)}}{(1-e^{k_{em}\tau})}\right)\right) & if\ t \le Tk0 \\ \dfrac{FDose\, k_m}{Tk0\,V_m\left(k-k_{em}\right)}\left(\dfrac{\left(e^{-kt}-1\right)e^{-k(t-Tk0)}}{k(1-e^{k\tau})}+\dfrac{\left(1-e^{-k_{em}t}\right)e^{-k_{em}(t-Tk0)}}{k_{em}(1-e^{k_{em}\tau})}\right) & if\ not \end{cases}$$

where C_{3TC} is the plasma concentration of 3TC, $C_{3TC\text{-}TP}$ the intracellular concentrations of the metabolite 3TC-TP and $k=k_e+k_m$.

These models were reparameterized using the apparent clearance of plasma NRTIs $Cl/F = k\,(V/F)$ and for their metabolite $Cl_m/F=k_{em}\,(V_m/F)$. Since AZT and 3TC are orally administrated, k_a for AZT or *Tk0* for 3TC and Cl/F, V/F were identifiable. Concerning metabolites, since no urinary concentration were available, only the parameters $(Cl_m/F)/k_m$ and $(V_m/F)/k_m$ were identifiable (21, 29). We could thus determined k_{em} as the ratio of both previous parameters and also the half-lives of

parent drugs and metabolites. We then computed intersubject variabilities for these derived parameters as the sum of the intersubject variability of the composing parameter as they were no covariance between random effects. We also deduced the relative standard error (RSE) of k_{em} using the delta method. More complex models in terms of number of compartment and ways of administration of the parent drug were tested whereas no saturable metabolism or such more complex phenomena were evaluated due to identification issue of the model.

For each joint model, an exponential model was used for intersubject variability where random effects were assumed to follow a normal distribution with zero mean and diagonal variance matrix. Since the MONOLIX software handles left censored data, AZT and 3TC plasma concentrations below LOQ were taken into account in the estimation step using the left censored LOQ (31). However, because of the complex assay techniques used to analyse intracellular measurement of AZT-TP and 3TC-TP, the data undetectable or below quantifiable limit were omitted. Several residual error models for each drug and for each moiety (i.e. additive, proportional, and combined) were investigated based on the Bayesian information criterion (BIC) (9, 23). We then built a model with random effects on all PK parameters. Model choice was based on the BIC and standard goodness-of-fit plots (observed concentrations versus predicted population and individual concentrations; population and individual weighted residuals versus predicted concentrations and versus time) for each drug and each moiety. For evaluation of the basic joint model, we performed a visual predictive check (VPC) with 5000 simulations to evaluate the basic model for each drug and its metabolite.

The effects of the following covariates were then evaluated: age, body mass index (BMI), body weight, creatinine clearance and albumin as continuous variables, co-administrated PI (Indinavir/Nelfinavir/Lopinavir), ritonavir intake, co-infection by hepatitis C or B virus (HCV/HBV), adherence as previously defined, gender and CDC classification for HIV infection The

continuous variables were centered to the median for model interpretation convenience. Missing continuous covariates were replaced with the median and patients with missing discrete covariates were discarded from the correspondent analysis. The effects of covariates on the empirical Bayes estimates (EBE) of each individual pharmacokinetic parameter from the basic model were tested with the Wilcoxon non-parametric test for categorical variables and the Spearman non-parametric test for continuous variables. The population covariate model was built with the covariates which were found to have an effect in this first step with a p-value < 0.2. A forward selection of these covariates for the population model was performed by use of the likelihood ratio test (LRT) with a significance threshold at $p < 0.05$. For each nested models, the likelihood ratio test can be applied by computing the log-likelihood by importance sampling using a Monte Carlo size of 20000. From this ascending method, a backward elimination procedure was performed to keep only significant covariates ($p < 0.05$) in the final model and to assess their p-values by use of LRT.

Relationships between plasma, intracellular AZT and 3TC concentration

Using joint models, the mean plasma concentration and the mean intracellular concentration at steady-state are given by $C_{mean} = \frac{Dose/\tau}{Cl/F}$ and $C_{mean,intra} = \frac{Dose/\tau}{Cl/V}\frac{1}{(Cl_m/F)/k_m}$, respectively. The mean metabolic ratio (*MMR)* is therefore expressed as $MMR = \frac{C_{mean,intra}}{C_{mean}} = \frac{V/F}{(Cl_m/F)/k_m}$.

Using estimated individual parameters in patients with both intracellular samples of AZT-TP and 3TC-TP, we first studied correlations between C_{mean} for AZT and 3TC, $C_{mean,intra}$ for AZT-TP and 3TC-TP as well as between MMR for AZT and 3TC. Then, for each drug, correlations between mean plasma and mean intracellular concentration were studied. We also investigated correlation between C_{mean} and $C_{mean,intra}$ and the covariates found for each final model, respectively to observe

their clinical relevance. The correlation tests were performed using the non-parametric Spearman test or the Wilcoxon non-parametric test according to the type of covariates. Tests have been performed using R software version 2.6.2.

RESULTS

Patients

Seventy-five patients (47 men, 28 women) of the 115 patients of the COPHAR2 ANRS 111 trial, received the combination of AZT/ 3TC. Among them, 27, 23 and 25 patients were respectively treated with indinavir, nelfinavir and lopinavir as PI. For two patients, plasma samples were missing. We therefore obtained plasma pharmacokinetic data for AZT and 3TC from 73 patients. Table I describes the main characteristics of the 73 patients included in the population analysis. We obtained a total of 280 AZT plasma concentrations and 287 for 3TC (a median of four samples per patient for AZT and 3TC). Among these 73 patients, only 62 patients had intracellular concentrations for both AZT-TP and 3TC-TP, 11 patients with four sampling times and other patients with three, two or one sample (a median of two samples per patient for AZT-TP and 3TC-TP).

Joint population modelling of AZT and intracellular AZT-TP

Among the 280 samples, 6% were below the LOQ for AZT in plasma. Figure 2A displays AZT and AZT-TP concentrations versus time. The concentrations of both compounds were adequately described by a one-compartment model with first-order absorption and elimination for AZT with an additional compartment for AZT-TP. Indeed, more complex models did not improve the results. Residual variabilities of AZT and AZT-TP were best depicted by an additive and a proportional error model, respectively. The available data were not sufficient to estimate k_a and we

had to fix the value of k_a to 2.86 h^{-1} which was obtained by Panhard et al. (29) in the population analysis of AZT and 3TC plasma concentrations originally from the COPHAR 1-ANRS 102 trial. Indeed, in that trial an early sampling times (0.5 h) after drug administration was performed. No sensitivity analyse was performed on this parameter as very few information is available during the absorption phase. Results showed no significant improvement when intersubject variability of $V_m/(Fkm)$ was added, so that no variability was assumed for that parameter. The population parameter estimates and their relative standard errors (RSE) are displayed in Table II. The residual variability for AZT-TP was 45%. The RSE for all parameters were correct. We derived the secondary parameter k_{em} equal to 0.063 h^{-1} with intersubject variability equal to those of $Cl_m/(Fkm)$. The mean half-lifes were 0.81 h and 10.73 h for AZT and AZT-TP compounds. The estimated intersubject variabilities, 94.8% and 58.4% respectively, were large for both mean half-lifes. VPC of AZT and AZT-TP are displayed in Fig. 2 and they show good evidence of the adequacy of the models.

Significant effects of adherence on V/F ($p = 0.021$) and of gender on Cl/F ($p = 0.022$) were found. The population parameters of this final model are given in Table II. An increase of 33% of the apparent clearance of AZT was observed for male. Apparent volume of distribution of AZT was increased by 55% for non-adherents patients.

Joint population modelling of 3TC and intracellular 3TC-TP

Three patients had plasma concentrations of 3TC at 12 h below the LOQ. Figure 2B shows 3TC and 3TC-TP concentrations versus time. A similar model that for AZT/AZT-TP, but with a zero order absorption best depicted concentrations of 3TC and its metabolite 3TC-TP. *Tk0* was estimated to 1.25 h. No variability on $V_m/(Fkm)$ was estimated. The best error models were an additive error model for 3TC and a proportional error model for 3TC-TP. Table III shows the population parameter estimates and their RSE in percent. Parameters are well estimated with RSE

lower than 20% except for $V_m/(Fkm)$ (47.6%). Important intersubject variability are estimated for $Tk0$ (74%) and $Cl_m/(Fk_m)$ (47.5%). The residual variability for 3TC-TP was 24.5%. We obtained k_{em} of 0.027 h^{-1} with an intersubject variability equal to 47.5%. 3TC and 3TC-TP have mean half-lifes equal to 2.97 h and 21.16 h with intersubject variabilities equal to 39.2% and 47.5% respectively. VPC are given in Fig. 2B for the joint 3TC/3TC-TP model and they show good evidence of the adequacy of the models.

Five covariates were included in the final model. We found a significant effect of ritonavir on $Tk0$ ($p = 0.04$). The apparent clearance (Cl/F) of 3TC was influenced significantly by age ($p = 0.001$), body-weight ($p = 0.007$) and by adherence ($p = 0.02$). An effect of gender on the apparent volume (V/F) of 3TC ($p = 0.001$) was also found. Duration of absorption of 3TC for a patient taking ritonavir, i.e. treated by lopinavir or indinavir as PI, was increased by 121%. 3TC apparent volume of distribution was increased by 23% in male patients. Each increase of 10 years of age from the median (34 years), the apparent clearance of 3TC decreased by 9% whereas the latter increases by 7% each increase of 10 kg from the median (68 kg). A decrease of 15% of the apparent clearance was observed for non-adherent patients.

Relationships between plasma, intracellular AZT and 3TC exposition and covariates

Median AZT and 3TC mean concentrations in plasma were 0.11 mg/L (IQR 0.1 - 0.18) and 0.51 mg/L (IQR 0.4 - 0.7), for the 62 subjects in whom both plasma and intracellular concentrations of AZT and 3TC were available. The median mean intracellular concentration was 0.17 mg/L (IQR 0.11 - 0.24) for AZT-TP and 58.1 mg/L (IQR 43.7 - 75.8) for 3TC-TP. Significant relationship was found between mean plasma concentration of AZT and 3TC ($r = 0.30$, $p = 0.016$) as well as between mean intracellular concentration ($r = 0.56$, $p<0.001$) (Fig 4). Significant relationship was

also found between mean AZT concentrations in plasma and mean intracellular concentrations of AZT-TP ($r = 0.35$, $p = 0.006$) and similarly for 3TC and 3TC-TP ($r = 0.48$, $p < 0.001$) (Fig 3).

Median MMR were 0.66 (IQR 0.46 - 1.16) for AZT/AZT-TP and 51.4 (IQR 38.6 - 68.7) for 3TC/ 3TC-TP. No relationship was found between MMR of AZT and MMR of 3TC which was higher.

Regarding the correlation with the covariates included in the final joint models, we found only a correlation between the mean plasma concentration of AZT and mean intracellular concentration of AZT-TP with the gender covariate ($p = 0.027$ and $p = 0.039$, respectively) (Fig 4). Median AZT mean concentration in plasma was 0.16 (IQR 0.10 - 0.21) for female (n=23) and 0.10 (IQR 0.07 – 0.15) for male patients (n=29). Similarly, median of AZT-TP mean concentration was higher in female patients than in men, when all mean AZT-TP concentrations were grouped by gender the median value was 0.19 (IQR 0.14 - 0.26) for female and 0.14 (IQR 0.08 - 0.23) for male. No other significant correlations were found.

DISCUSSION

For the first time, joint models were developed for the analysis of AZT and 3TC plasma concentrations and for their respective active metabolite AZT-TP and 3TC-TP intracellular concentrations. Concentrations of AZT and of AZT-TP were satisfactorily described by a one compartment model with first-order absorption and elimination for AZT, with an additional compartment for AZT-TP linked with a first order rate constant. Regarding 3TC and 3TC-TP, the same compartment model but with a zero order absorption fitted adequately the data. The design used in the COPHAR 2 ANRS 111 trial has been originally planned to study pharmacokinetics of PI. Due to the absence of any sampling times during the absorption phase, we could not estimate the

parameter k_a of AZT, which has thus been fixed to 2.86 h^{-1}. This value was obtained by Panhard et al. (29) in the COPHAR1-ANRS 102 trial where the design included a sample in the absorption phase. We found apparent clearances of 200 $L.h^{-1}$ and 22 $L.h^{-1}$ for AZT and 3TC with estimated intersubject variabilities of 54% and of 31%, respectively. Mean half-lifes of AZT and 3TC were equal to 0.8 h and 2.9 h, respectively and intersubject variabilities of 94.8% and 39.2% were derived. Values of the parameters obtained in the present study for plasma AZT and 3TC were within the range of those estimated previously. For instance, regarding half-life values in HIV patients, they are consistent with previously reported values: for AZT, 1.2 to 4 h (14, 33) and for 3TC, 3.8 h (14).

The pharmacokinetics of the AZT-TP and 3TC-TP metabolite has already been studied by using only usual statistics due to the lack of information to build an adequate intracellular model. The use of a joint population model is optimum to obtain accurate pharmacokinetic parameters for metabolites instead of sequential analysis of each compound and can deal with sparse measurements. For AZT-TP and 3TC-TP, large intersubject variabilities of 58.4% and 47.5%, were found for $Cl_m/(Fk_m)$. Intracellular mean half-lifes for AZT-TP and 3TC-TP are 10.7 h and 21.2 h, with respectively, 58.4% and 47.5% for the intersubject variabilities. Published data in HIV infected patients show that the reported intracellular half-lifes are rather variable. For AZT-TP, they are between 2 h and 25 h (4, 14, 18, 33) and, for 3TC-TP between 10 h and 22 h (1, 14, 26). The differences between the reported intracellular half-lifes can be explained by several factors. Most published studies were based on single measurements collected at variable times during a dosing interval, which can lead to large fluctuations in measurements. Then, quantification of intracellular concentrations is technically and analytically challenging and there is still the need for a standardised method (6). As most studies, we found that intracellular active metabolites AZT-TP and 3TC-TP persist within the cells for a longer period of time compared to plasma measurement pointing up once daily dosing for the NRTI compared to twice daily dosing (Fig 5).

To develop these joint models, for plasma concentrations, we have included the measurements below the LOQ for plasma concentration and taken into account this left censoring in the MONOLIX software. Samson et al. (31) have shown that this proposed method is less biased than the usual methods of handling such data i.e. deletion of all censored data points, or imputation of LOQ/2 to the first point below the limit and deletion of the following points. However for AZT-TP and 3TC-TP concentrations, the problem is different. Indeed, due to the mixture of two difference assay techniques, it is not possible to define an upper limit like a "LOQ" for these data. That is why, for the estimation step, we omitted the intracellular data when they were undetectable or under the limit of quantification for one of the assay technique used. Regarding the mixture of the two difference assay techniques, there is one for the count of cells and one for the intracellular metabolite concentration. Since the number of cells normalises intracellular concentration, the counting of cell is a critical step in the process of intracellular assay. In the present study, the cell numbering was performed according to a validated biochemical assay (8) and the concentration was expressed as amounts per 10^6 cells and had been converted in amount per volume on the approximation that the PBMC volume is 0.2 pL in order to compare intracellular and plasma concentrations. Another often used value for the PBMC volume is 0.4 pL (19). Nevertheless, this may be questionable as it varies according to the state of the cells (quiescent or stimulated) or to the nature of the cells (cell volume of human lymphoblast : 2.1 pL) (36). Even if this point is largely discussed, the PBMC volume is only a scale factor and thus does not modify our results.

A major aim of population pharmacokinetics is to determine which measurable factors can cause changes in the dose-concentration relationship. We found an increase by 55% of the apparent volume of distribution for non-adherent patients. Similarly, adherence was shown to decrease the apparent clearance of 3TC by 15% for non-adherent patients. We thus found a systemic correlation between adherence effect and apparent clearance (Cl/F) and apparent volume of distribution (V/F).

We assumed that the adherence might affect the pharmacokinetics of the drugs by means of the bioavailability. Adherence is the major component of clinical variability in response to drug treatment, low adherence to antiretroviral drugs may lead to a sub-optimal therapy (20) and emergence of resistant virus. We found an increase of the 3TC duration absorption for patient taking ritonavir. Pharmacokinetic interaction studies with ritonavir have not been reported for 3TC. A hypothesis for the raise of the duration of absorption could be that the patients receiving ritonavir were fed because absorption of 3TC has been shown to be slower in fed compared with fasted patients, which could be in agreement with the increased of Tk0 (2, 27). We can not confirm this hypothesis on our data because only patients receiving nelfinavir getting recommended dietary guidelines oral and written. Panhard et al. (29) found an increase of the absorption duration in patients receiving nelfinavir and also an effect of the age and the body weight on this parameter. In the present study, we observed a slight but opposite influence of the age and body-weight on the apparent clearance of 3TC as found in Moore et al. study (28).

An effect of the gender on the apparent volume of 3TC was underlined as well as on the apparent clearance of AZT. Furthermore, we found a significant correlation between gender covariate and mean plasma concentration of AZT as well as with mean intracellular concentration of AZT-TP, pointing out the clinical relevance of the gender effect. Women had higher AZT and AZT-TP concentrations compared with men. It is in agreement with the effect found on the apparent clearance for AZT, which is increased of 33% for the male, eliminating quickly AZT concentrations and as a result reducing AZT-TP concentrations. Anderson et al. (1) found a similar gender effect on intracellular concentrations of AZT-TP and 3TC-TP in opposite to the one found by Aweeka et al. (4) for AZT-TP. This discrepancy may be explained in that the latter study 20 women were enrolled (compared with only 4 women) and variable AZT doses were permitted. Stretcher et al. (34) provided gender related-differences in AZT-TP using AUC estimates in sixteen man and five

women. The findings indicated the higher exposure of women. Current evidence, though limited, suggested the existence of gender disparity and thus provided motivation to conduct further investigations of intracellular AZT pharmacokinetics and pharmacodynamics in men and women, a group for which historically experiences showed high rates of serious toxicities (37).

Mean metabolic ratio of 3TC (median 51.4) is much larger than the mean metabolic ratio of AZT (median 0.66). The intersubject variability of MMR was 96.8% for AZT and 32.8% for 3TC, which is far lower than AZT. 3TC-TP concentrations tended to be higher than AZT-TP concentrations whereas the median mean plasma concentrations in plasma for both parent drugs are in the same range. Using descriptive statistics, Moore et al. (25) found mean intracellular/plasma concentrations ratios of 0.05% and 3%, for AZT and 3TC, respectively. If we compare the MMR of 3TC and AZT by calculating the ratio MMR AZT/MMR 3TC they are in the same range (0.016 and 0.013 in Moore et al. and in this study, respectively).

In this study including patients with dual combination of AZT and 3TC, a significant statistical correlation between mean plasma concentration of AZT and 3TC was found likewise between mean intracellular concentration of AZT-TP and 3TC-TP. Relationships between mean plasma and intracellular concentration were also highlighted both for AZT and for 3TC. Although significant, the correlations are low (AZT: $r^2 = 0.12$; 3TC: $r^2 = 0.23$). Identical results were found in Hoggard et al. (22) for AZT, in Fletcher et al. (17) for 3TC and Durand-Gasselin et al. (15) for both drugs. Several published studies have also tested these correlations without significant results for AZT and AZT-TP (5, 14, 17, 30, 34, 35) but they were of limited size. The new finding on the relationship between plasma and intracellular concentrations of both drugs suggest the use of plasma concentrations for monitoring AZT and 3TC treatment. In addition, plasma concentrations need a simpler assay technique than intracellular concentrations. The large difference of intracellular triphosphates between AZT and 3TC (i.e. very different MMR values) demonstrate that there are

substantial differences in the extent of conversion of these antiviral agents especially for cellular transport and metabolism. A further step will be to study relationships between intracellular concentrations and antiviral response through modelling (24) to really study the potential of intracellular concentrations as a therapeutic determinant of efficacy or toxicity of antiretroviral therapy as observed in previous studies (1, 3, 17, 25, 33).

In conclusion, a joint pharmacokinetic model was developed for AZT and its active metabolite AZT-TP as well as for 3TC and 3TC-TP allowing to obtain accurate estimation on metabolite parameters but with a large between patients variability. A very long half-life is observed for AZT-TP and 3TC-TP supporting a once daily regimen for both AZT and 3TC. The clinically relevance of the gender effect on AZT pharmacokinetics may have implications for drug efficacy and toxicity in men and women. Last, the correlation found between plasma and intracellular concentration for both AZT and 3TC, even if it is limited, supports the necessity to measure intracellular concentrations for antiviral activity.

Acknowledgements

The authors thank the study participants, the participating clinicians and the Agence de Recherche Nationale sur le SIDA for financial support.

References

1. **Anderson, P. L., T. N. Kakuda, S. Kawle, and C. V. Fletcher.** 2003. Antiviral dynamics and sex differences of zidovudine and lamivudine triphosphate concentrations in HIV-infected individuals. Aids **17:**2159-2168.
2. **Angel, J., E. Hussey, S. Hall, K. Donn, D. Morris, J. McCormack, J. Montaner, and J. Ruedy.** 1993. Pharmacokinetics of GR109714X (3TC) HIV infected patients when administered with and without food. Drug Invest **6:**70-74.
3. **Aweeka, F. T., M. Kang, J. Y. Yu, P. Lizak, B. Alston, and R. T. Chung.** 2007. Pharmacokinetic evaluation of the effects of ribavirin on zidovudine triphosphate formation: ACTG 5092s Study Team. HIV Med **8:**288-294.
4. **Aweeka, F. T., S. L. Rosenkranz, Y. Segal, R. W. Coombs, A. Bardeguez, L. Thevanayagam, P. Lizak, J. Aberg, and D. H. Watts.** 2006. The impact of sex and contraceptive therapy on the plasma and intracellular pharmacokinetics of zidovudine. Aids **20:**1833-1841.
5. **Barry, M. G., S. H. Khoo, G. J. Veal, P. G. Hoggard, S. E. Gibbons, E. G. Wilkins, O. Williams, A. M. Breckenridge, and D. J. Back.** 1996. The effect of zidovudine dose on the formation of intracellular phosphorylated metabolites. AIDS **10:**1361-1367.
6. **Bazzoli, C., V. Jullien, C. Le Tiec, E. Rey, F. Mentré, and A. M. Taburet.** 2010. Intracellular Pharmacokinetics of Antiretroviral Drugs in HIV-Infected Patients, and their Correlation with Drug Action. Clinical pharmacokinetics **49:**17-45.
7. **Becher, F., A. Pruvost, J. Gale, P. Couerbe, C. Goujard, V. Boutet, E. Ezan, J. Grassi, and H. Benech.** 2003. A strategy for liquid chromatography/tandem mass spectrometric assays of intracellular drugs: application to the validation of the triphosphorylated anabolite of antiretrovirals in peripheral blood mononuclear cells. J Mass Spectrom **38:**879-890.
8. **Benech, H., F. Theodoro, A. Herbet, N. Page, D. Schlemmer, A. Pruvost, J. Grassi, and J. R. Deverre.** 2004. Peripheral blood mononuclear cell counting using a DNA-detection-based method. Anal Biochem **330:**172-174.
9. **Bertrand, J., E. Comets, and F. Mentre.** 2008. Comparison of model-based tests and selection strategies to detect genetic polymorphisms influencing pharmacokinetic parameters. Journal of biopharmaceutical statistics **18:**1084-1102.

10. **Bertrand, J., J. M. Tréluyer, X. Panhard, A. Tran, S. Auleley, E. Rey, D. Salmon-Céron, X. Duval, and F. Mentré.** 2009. Influence of pharmacogenetics on indinavir disposition and short-term response in HIV patients initiating HAART. Eur J Clin Pharmacol **65:**667-678.

11. **Carrieri, P., V. Cailleton, V. Le Moing, B. Spire, P. Dellamonica, E. Bouvet, F. Raffi, V. Journot, and J. P. Moatti.** 2001. The dynamic of adherence to highly active antiretroviral therapy: results from the French National APROCO cohort. J Acquir Immune Defic Syndr **28:**232-239.

12. **Chapman, E. H., A. S. Kurec, and F. R. Davey.** 1981. Cell volumes of normal and malignant mononuclear cells. J Clin Pathol **34:**1083-1090.

13. **Compain, S., L. Durand-Gasselin, J. Grassi, and H. Benech.** 2007. Improved method to quantify intracellular zidovudine mono- and triphosphate in peripheral blood mononuclear cells by liquid chromatography-tandem mass spectrometry. J Mass Spectrom **42:**389-404.

14. **Dumond, J. B., Y. S. Reddy, L. Troiani, J. F. Rodriguez, A. S. Bridges, S. A. Fiscus, G. J. Yuen, M. S. Cohen, and A. D. Kashuba.** 2008. Differential extracellular and intracellular concentrations of zidovudine and lamivudine in semen and plasma of HIV-1-infected men. J Acquir Immune Defic Syndr **48:**156-162.

15. **Durand-Gasselin, L., A. Pruvost, A. Dehee, G. Vaudre, M. D. Tabone, J. Grassi, G. Leverger, A. Garbarg-Chenon, H. Benech, and C. Dollfus.** 2008. High levels of zidovudine (AZT) and its intracellular phosphate metabolites in AZT- and AZT-lamivudine-treated newborns of human immunodeficiency virus-infected mothers. Antimicrob Agents Chemother **52:**2555-2563.

16. **Duval, X., F. Mentré, E. Rey, S. Auleley, G. Peytavin, M. Biour, A. Métro, C. Goujard, A. N. Taburet, C. Lascoux, X. Panhard, J. M. Tréluyer, D. Salmon-Céron, and the Cophar 2 study group.** 2009. Benefit of therapeutic drug monitoring of protease inhibitors in HIV-infected patients depends on PI used in HAART Regimen – ANRS 111 trial. Fundam Clin Pharmacol **23:**491-500.

17. **Fletcher, C. V., S. P. Kawle, T. N. Kakuda, P. L. Anderson, D. Weller, L. R. Bushman, R. C. Brundage, and R. P. Remmel.** 2000. Zidovudine triphosphate and lamivudine triphosphate concentration-response relationships in HIV-infected persons. Aids **14:**2137-2144.

18. **Flynn, P. M., J. Rodman, J. C. Lindsey, B. Robbins, E. Capparelli, K. M. Knapp, J. F. Rodriguez, J. McNamara, L. Serchuck, B. Heckman, and J. Martinez.** 2007. Intracellular pharmacokinetics of once versus twice daily zidovudine and lamivudine in adolescents. Antimicrob Agents Chemother **51:**3516-3522.

19. **Gao, W. Y., A. Cara, R. C. Gallo, and F. Lori.** 1993. Low levels of deoxynucleotides in peripheral blood lymphocytes: a strategy to inhibit human immunodeficiency virus type 1 replication. Proc Natl Acad Sci U S A **90:**8925-8928.

20. **Gifford, A. L., J. E. Bormann, M. J. Shively, B. C. Wright, D. D. Richman, and S. A. Bozzette.** 2000. Predictors of self-reported adherence and plasma HIV concentrations in patients on multidrug antiretroviral regimens. J Acquir Immune Defic Syndr **23:**386-395.

21. **Hirt, D., F. Mentré, A. Tran, E. Rey, S. Auleley, D. Salmon, X. Duval, and J. M. Treluyer.** 2008. Effect of CYP2C19 polymorphism on nelfinavir to M8 biotransformation in HIV patients. Br J Clin Pharmacol **65:**548-557.

22. **Hoggard, P. G., J. Lloyd, S. H. Khoo, M. G. Barry, L. Dann, S. E. Gibbons, E. G. Wilkins, C. Loveday, and D. J. Back.** 2001. Zidovudine phosphorylation determined sequentially over 12 months in human immunodeficiency virus-infected patients with or without previous exposure to antiretroviral agents. Antimicrob Agents Chemother **45:**976-980.

23. **Lavielle, M., and F. Mentre.** 2007. Estimation of population pharmacokinetic parameters of saquinavir in HIV patients with the MONOLIX software. Journal of pharmacokinetics and pharmacodynamics **34:**229-249.

24. **Lavielle, M., A. Samson, A. Karina Fermin, and F. Mentré.** Maximum Likelihood Estimation of Long-Term HIV Dynamic Models and Antiviral Response. Biometrics.

25. **Moore, J. D., E. P. Acosta, V. A. Johnson, R. Bassett, J. J. Eron, M. A. Fischl, M. C. Long, D. R. Kuritzkes, and J. P. Sommadossi.** 2007. Intracellular nucleoside triphosphate concentrations in HIV-infected patients on dual nucleoside reverse transcriptase inhibitor therapy. Antivir Ther **12:**981-986.

26. **Moore, K. H., J. E. Barrett, S. Shaw, G. E. Pakes, R. Churchus, A. Kapoor, J. Lloyd, M. G. Barry, and D. Back.** 1999. The pharmacokinetics of lamivudine phosphorylation in peripheral blood mononuclear cells from patients infected with HIV-1. Aids **13:**2239-2250.

27. **Moore, K. H., S. Shaw, A. L. Laurent, P. Lloyd, B. Duncan, D. M. Morris, M. J. O'Mara, and G. E. Pakes.** 1999. Lamivudine/zidovudine as a combined formulation tablet:

bioequivalence compared with lamivudine and zidovudine administered concurrently and the effect of food on absorption. J Clin Pharmacol **39:**593-605.

28. **Moore, K. H., G. J. Yuen, E. K. Hussey, G. E. Pakes, J. J. Eron, Jr., and J. A. Bartlett.** 1999. Population pharmacokinetics of lamivudine in adult human immunodeficiency virus-infected patients enrolled in two phase III clinical trials. Antimicrob Agents Chemother **43:**3025-3029.
29. **Panhard, X., M. Legrand, A. M. Taburet, B. Diquet, C. Goujard, and F. Mentré.** 2007. Population pharmacokinetic analysis of lamivudine, stavudine and zidovudine in controlled HIV-infected patients on HAART. Eur J Clin Pharmacol **63:**1019-1029.
30. **Rodman, J. H., P. M. Flynn, B. Robbins, E. Jimenez, A. D. Bardeguez, J. F. Rodriguez, S. Blanchard, and A. Fridland.** 1999. Systemic pharmacokinetics and cellular pharmacology of zidovudine in human immunodeficiency virus type 1-infected women and newborn infants. J Infect Dis **180:**1844-1850.
31. **Samson, A., F. Mentré, and M. Lavielle.** 2006. Extension of the SAEM algorithm to left-censored data in nonlinear mixed-effects model: application to HIV dynamics model. Comput Stat Data Anal **51:**1562-1574.
32. **Segel, G. B., G. R. Cokelet, and M. A. Lichtman.** 1981. The measurement of lymphocyte volume: importance of reference particle deformability and counting solution tonicity. Blood **57:**894-899.
33. **Stretcher, B. N., A. J. Pesce, P. T. Frame, K. A. Greenberg, and D. S. Stein.** 1994. Correlates of zidovudine phosphorylation with markers of HIV disease progression and drug toxicity. Aids **8:**763-769.
34. **Stretcher, B. N., A. J. Pesce, P. T. Frame, and D. S. Stein.** 1994. Pharmacokinetics of zidovudine phosphorylation in peripheral blood mononuclear cells from patients infected with human immunodeficiency virus. Antimicrob Agents Chemother **38:**1541-1547.
35. **Stretcher, B. N., A. J. Pesce, P. E. Hurtubise, and P. T. Frame.** 1992. Pharmacokinetics of zidovudine phosphorylation in patients infected with the human immunodeficiency virus. Ther Drug Monit **14:**281-285.
36. **Traut, T. W.** 1994. Physiological concentrations of purines and pyrimidines. Mol Cell Biochem **140:**1-22.
37. **Umeh, O. C., and J. S. Currier.** 2005. Sex Differences in HIV: Natural History, Pharmacokinetics, and Drug Toxicity. Current infectious disease reports **7:**73-78.

38. **World Health Organization** November 30 2009, posting date. New WHO Recommendations: Antiretroviral therapy for adults and adolescents. [Online.]

Figure legends

Fig 1.

Schematic representation of joint pharmacokinetic compartment models for the simultaneous prediction of AZT and 3TC concentrations and their active intracellular metabolite concentrations. AZT (resp. 3TC) in compartment 1 underwent irreversible biotransformation into AZT-TP (resp. 3TC-TP) in compartment 2. D ; dose; F: bioavailability of parent drug; k_a: first order absorption rate constant of AZT; $Tk0$: zero order absorption duration for 3TC; k_m: first order metabolism rate constant; k_e: first order elimination rate constant for parent drug; V: volume of distribution of the parent drug; V_m: volume of distribution of the metabolite; k_{em}: first order elimination rate constant for the metabolite.

Fig 2.

Visual predictive checks of basic joint population PK model for AZT (left) and AZT-TP (right) at steady-state for 300 mg b.i.d of AZT (A) and observed plasma concentrations of AZT (left) and intracellular concentrations of AZT-TP (right) (A) versus time. Visual predictive checks of basic joint population PK model for 3TC (left) and 3TC-TP (right) at steady-state for 150 mg b.i.d of 3TC (B) and observed plasma concentrations of 3TC (left) and intracellular concentrations of 3TC-TP (right) (B) versus time. The dashed lines are the median predictions and the shaded area is the 90% prediction intervals. Intracellular concentrations of AZT-TP and 3TC-TP expressed from the assay in fmol/L have been transformed in mg/L using the following molar mass : $M_{AZT\text{-}TP}$ = 507 g/mol and $M_{3TC\text{-}TP}$=469 g/mol.

Fig 3.

Relationship between mean plasma concentration of AZT and 3TC (A); between mean intracellular concentration of AZT-TP and 3TC-TP (B); between mean plasma concentration of AZT and mean intracellular concentrations of AZT-TP (C); between mean plasma concentration of 3TC and mean intracellular concentration of 3TC-TP (D).

Fig 4.

Relationship between mean plasma concentration of AZT and the gender covariate (A); between mean intracellular concentration of AZT-TP and the gender covariate (B).

Fig 5.

Predicted plasma concentrations of AZT (left) and intracellular concentrations of AZT-TP (right) at steady state for 600 mg q.d (grey line) and 300 mg b.i.d of AZT (A) and plasma concentrations of 3TC (left) and intracellular concentrations of 3TC-TP (right) at steady state for 300 mg q.d (black line) and 150 mg b.i.d. of 3TC (B). The dashed lines and the solid lines represent the 90% prediction intervals and the median predictions, respectively, obtained from Monte Carlo simulation with 3000 individuals using the parameters presented in Table II and Table III.

Tables

Table I. Characteristics of the 73 patients receiving AZT and 3TC included in the population analyses

	Median (range)
Age (years)	34.0 (21-59)
BMI(kg/m^2)	22.8 (17.4-35.8)
Weight (kg)	68.0 (50-103)
Creatinine clearance (μmol/L) [a]	81.0 (51-131)
Albumin (g/L) [b]	40 (25.5-533)
	Number of patients (%)
Gender (male/female)	46 (63.0) / 27 (27.0)
CDC classification for HIV infection (A or B/C)	53 (72.6) / 20 (27.4)
Co-infection HCB/HCV (yes/no)	9 (12.3) / 64 (87.7)
Protease inhibitor (Indinavir/Nelfinavir/Lopinavir)	27 (37.0) / 21 (28.8) / 25 (34.2)
Ritonavir (yes/no)	52 (71.2) / 21 (28.8)
Good adherence (yes/no)	31 (42.5) / 42 (57.5)
ABCB1 exon 26 (CC / CT / TT) [d]	26 (37.7) / 37(53.6) / 6 (8.7)
ABCB1 exon 21 (GG / GT / TT) [d]	44 (62.0) / 20 (28.1) / 7 (9.9)
CYP3A5 (4*1 / 3*1 / ≤2*1) [d]	16 (21.9) / 21 (28.8) / 36 (49.3)
CYP3A4*1B (*1A*1A / *1A*1B / *1B *1B) [d]	34 (47.9) / 13 (18.3) / 24 (33.8)

[a] Three patients had this information missing

[b] Ten patients had this information missing

[c] Thirteen patients had this information missing

[d] Two patients had missing information for all genotypes; in addition two patients had missing genotype for ABCB1 exon 26

Table II. Population pharmacokinetic parameters of AZT and AZT-TP for the basic and final model

		Basic model		Final model	
Compounds	Parameters[a]	Estimates	RSE (%)	Estimates	RSE (%)
AZT					
	k_a (h^{-1})	2.86 (fixed)	-	2.86 (fixed)	-
	Cl/F (L/h)	200	6.3	168	6.3
	$\beta_{Cl/F}^{Male}$	-	-	0.28	43.7
	V/F (L)	234	9.4	182	13.8
	$\beta_{V/F}^{Non-adh}$	-	-	0.44	41.3
	$\omega_{Cl/F}$ (%)	54.4	9.3	52.4	9.7
	$\omega_{V/F}$ (%)	77.7	10.8	73.8	11.2
	σ_{AZT} (mg/L)	0.05	33.6	0.05	33.7
AZT-TP					
	$Cl_m/(Fk_m)$ (L)	322	10.1	326	10.2
	$V_m/(Fk_m)$ (L/h)	$5.14\ 10^3$	21.5	$5.16\ 10^3$	23.9
	k_{em}[b] (h^{-1})	0.064	18.4	0.063	18.3
	$\omega_{Cl_m/(Fk_m)}$ (%)	58.4	15.6	58.3	15.5
	σ_{AZT-TP} (%)	45.4	9.0	45.1	9.0

[a] RSE, relative standard error (standard error of estimate divided by estimate and multiply by 100); ω, coefficient of variation for intersubject variability; σ, parameters of error model.

[b] Derived secondary parameter.

Table III. Population pharmacokinetic parameters of 3TC and 3TC-TP for the basic and final model

		Basic model		Final model	
Compounds	Parameters[a]	Estimates	RSE (%)	Estimates	RSE (%)
3TC					
	$Tk0$ (h)	1.25	11.8	0.71	36.8
	$\beta_{Tk0}^{With-rito}$	-	-	0.77	48.7
	Cl/F (L/h)	22.10	3.9	24.8	3.9
	$\beta_{Cl/F}^{Age}$	-	-	-0.01	31.7
	$\beta_{Cl/F}^{BWeight}$	-	-	0.007	38.2
	$\beta_{Cl/F}^{Non-adh}$	-	-	-0.16	44.3
	V/F (L)	94.80	3.7	80.9	5.3
	$\beta_{V/F}^{Male}$	-	-	0.21	31.1
	ω_{Tk0} $(\%)$	74.1	12.1	62.4	12.1
	$\omega_{Cl/F}$ $(\%)$	31.1	9.8	28.3	10.3
	$\omega_{V/F}$ $(\%)$	24.0	13.5	19.5	7.4
	σ_{3TC} (mg/L)	0.13	6.0	0.13	6.1
3TC-TP					
	$Cl_m/(Fk_m)$ (L)	1.88	6.8	1.82	6.6
	$V_m/(Fk_m)$ (L/h)	63.73	47.6	69.14	41.2
	k_{em}[b] (h^{-1})	0.027	49.3	0.026	45.7
	$\omega_{Clm/(Fkm)}$ $(\%)$	47.5	11.2	42.3	11.9
	σ_{3TC-TP} $(\%)$	24.5	7.7	25.0	8.0

[a] RSE, relative standard error (standard error of estimate divided by estimate and multiply by 100); ω, coefficient of variation for intersubject variability and σ, parameters of error model.

[b] Derived secondary parameter.

Fig 1.

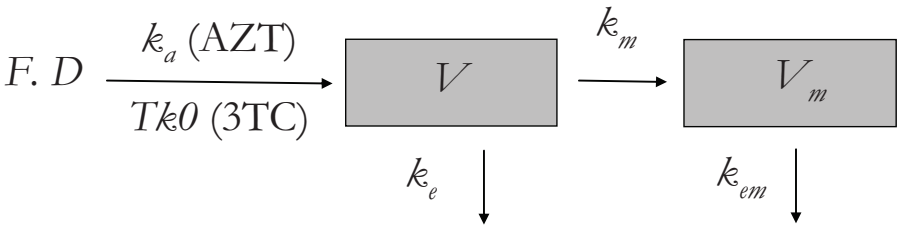

Fig 2.

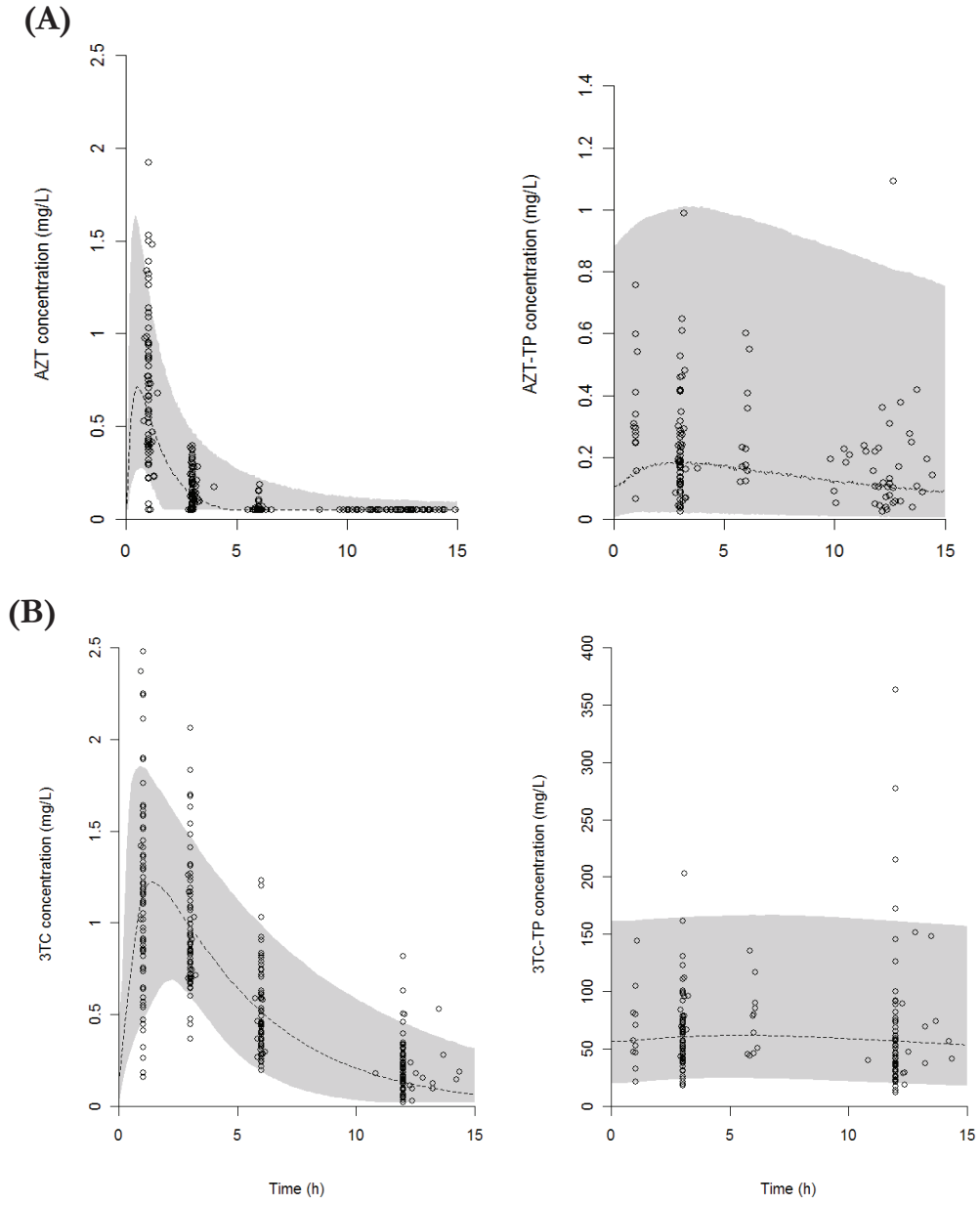
(A)
AZT concentration (mg/L)
AZT-TP concentration (mg/L)
(B)
3TC concentration (mg/L)
3TC-TP concentration (mg/L)
Time (h)
Time (h)

Fig 3.

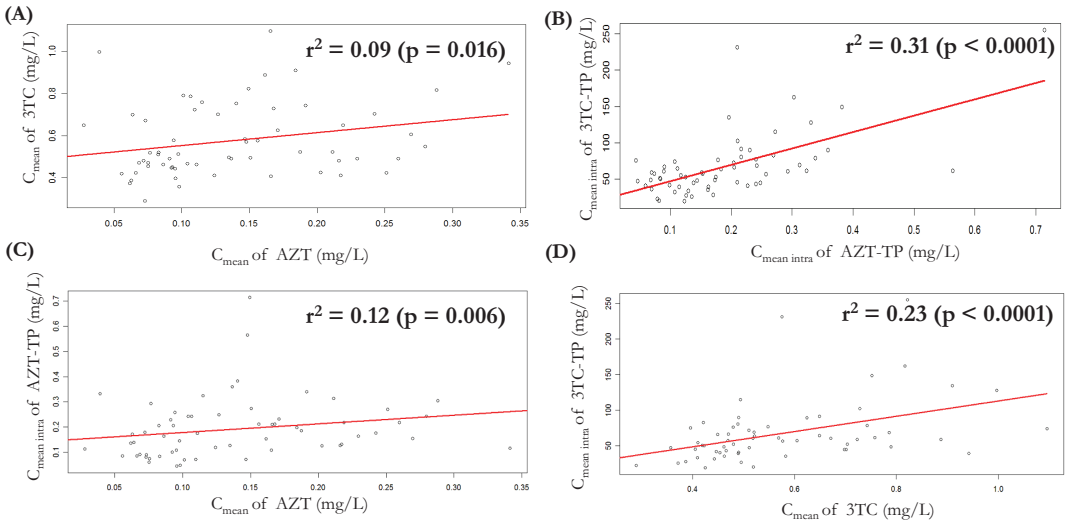
(A)
r² = 0.09 (p = 0.016)
C mean of 3TC (mg/L)
C mean of AZT (mg/L)
(B)
r² = 0.31 (p < 0.0001)
C mean intra of 3TC-TP (mg/L)
C mean intra of AZT-TP (mg/L)
(C)
r² = 0.12 (p = 0.006)
C mean intra of AZT-TP (mg/L)
C mean of AZT (mg/L)
(D)
r² = 0.23 (p < 0.0001)
C mean intra of 3TC-TP (mg/L)
C mean of 3TC (mg/L)

Fig 4.

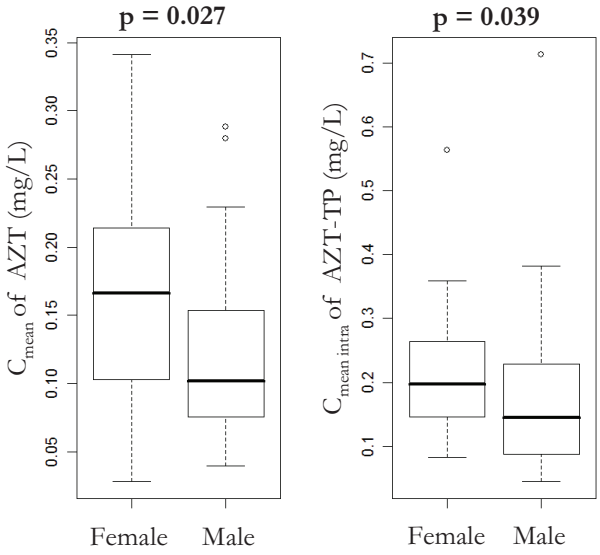
p = 0.027
p = 0.039
C_{mean} of AZT (mg/L)
$C_{mean\ intra}$ of AZT-TP (mg/L)
0.05
0.10
0.15
0.20
0.25
0.30
0.35
0.1
0.2
0.3
0.4
0.5
0.6
0.7
Female
Male
Female
Male

Fig 5.

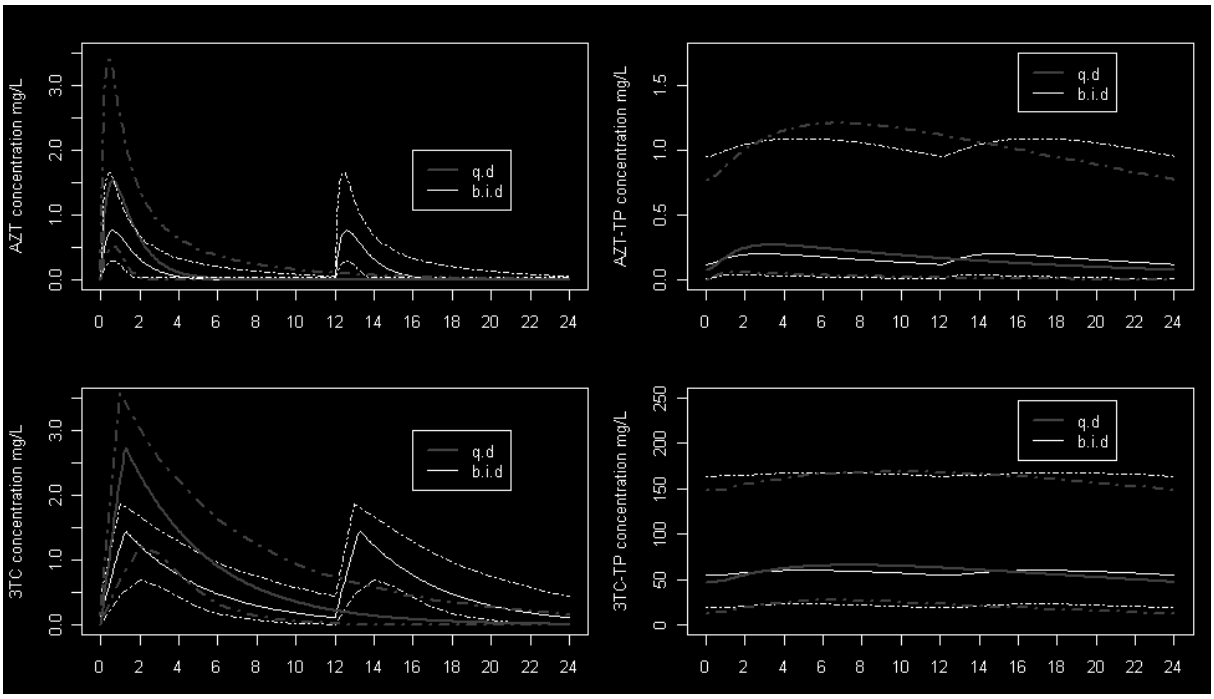
AZT concentration mg/L
AZT-TP concentration mg/L
3TC concentration mg/L
3TC-TP concentration mg/L
q.d
b.i.d